Hypervalent Iodine-Mediated Styrene Hetero- and Homodimerizations Initiation Proceed with Two-Electron Reductive Cleavage

Aqeel A. Hussein,[1,2]* Ahmed Al-Yasari [3,4‡] and Yumiao Ma[5‡]

[1] College of Dentistry, University of Al-Ameed, Karbala PO Box 198, Iraq.

[2] School of Chemistry, University of Southampton, Southampton, Hampshire, SO17 1BJ, United Kingdom.

[3] School of Chemistry, University of East Anglia, Norwich, NR4 7TJ, United Kingdom.

[4] Department of Chemistry, Faculty of Sciences, University of Kerbala, Kerbala, Iraq.

[5] BSJ Institute, Haidian, Beijing, 100084, People's Republic of China

Abstract

A mechanistic insight into the hetero- and homodimerizations (HETD and HOMD) of styrenes promoted by hypervalent iodine reagents (HVIRs; **DMP** and **PIDA**) and facilitated by HFIP to yield all *trans* cyclobutanes is reported using density functional theory (DFT) calculations. The reaction is initiated with two-electron reductive cleavage of two I─O bond cleavages, affording I(III) (iodinane) and I(I) (iodobenzene) product with DMP and PIDA as oxidant, respectively. The resulting acetate groups are stabilized by the solvent HFIP through strong hydrogen bonding interaction, which promotes the electron transfer process. The initialization involving one-electron transfer was found to be highly unfavored, especially for the PIDA system. At this point, we found that two-electron process is the key initialization process, which is in accordance with literature report on alcohol oxidation. The reaction rate is determined by the initialization step: For I(III), the initiation is thermodynamically endergonic, whereas the endergonicity for I(V) is modest. The difference in reactivity is explained by the difference LUMO energies. Upon initialization, the reaction proceeds through a stepwise [2+2] pathway, involving a radical-cationic π-π stacked intermediate, either hetero- or homodimerized. DFT results supported by quasiclassical molecular dynamics simulations show that HOMD is dynamically competing pathway to HETD although the latter is relatively faster, in accordance with experimental observations.

Introduction

Stereoselective approaches to substituted cyclobutanes have been captivated by organic chemists to be of high interest despite of its challenging requirements.[1, 2] Due to the fact that these cyclobutane rings exist in many bioactive natural products (Figure 1-a),[3-5] the need for such efficient, reliable, and benign synthesis methods is still under developing strategies to get a purely chiral strained carbocycle. Regardless the many different synthetic methodologies appeared in literatures to access cyclobutanes,[6-11] the olefin dimerization via oxidative manners, which involves an active radical cation intermediate formation, represents a helpful and promising tactic to reach. The olefin dimerization was firstly reported by Ledwith[12, 13] and Bauld,[14-16]. In this regard, metal complexes[17] and organic [18, 19] photoredox catalysis have been applied to promote such a nice cyclization.[20-28] Recently, a major contribution to this field has been exploited by using catalytic amounts of HVIR [29, 30] in HFIP to investigate a stereoselective functionalization of alkenes.[31-33] The HFIP has been shown to be a unique solvent due its significant role of hydrogen bonding [34-36] that enables the HVIR to act as single electron oxidants.[37-40] Based on the utility of the HVIR/HFIP, Donohoe and co-workers have developed a diastereoselective [2+2] cycloaddition of alkenes with remarkable results (Figure 1-b).[41, 42] The mechanism proposed involves a SEO of styrene **1** to a radical cation $\mathbf{1}^{+}$ by HVIR followed by either HOMD, where dimerization proceeds with another molecule of styrene **1** in the presence of I(III) **PIDA**, or HETD, where dimerization proceeds with a different alkene **2** in the presence of I(V) **DMP**, to give the all *trans* cyclobutane product **3** after the re-addition of an electron to the product. The presence of a *p*-methoxy group plays an important role in the success of a styrene toward dimerization.

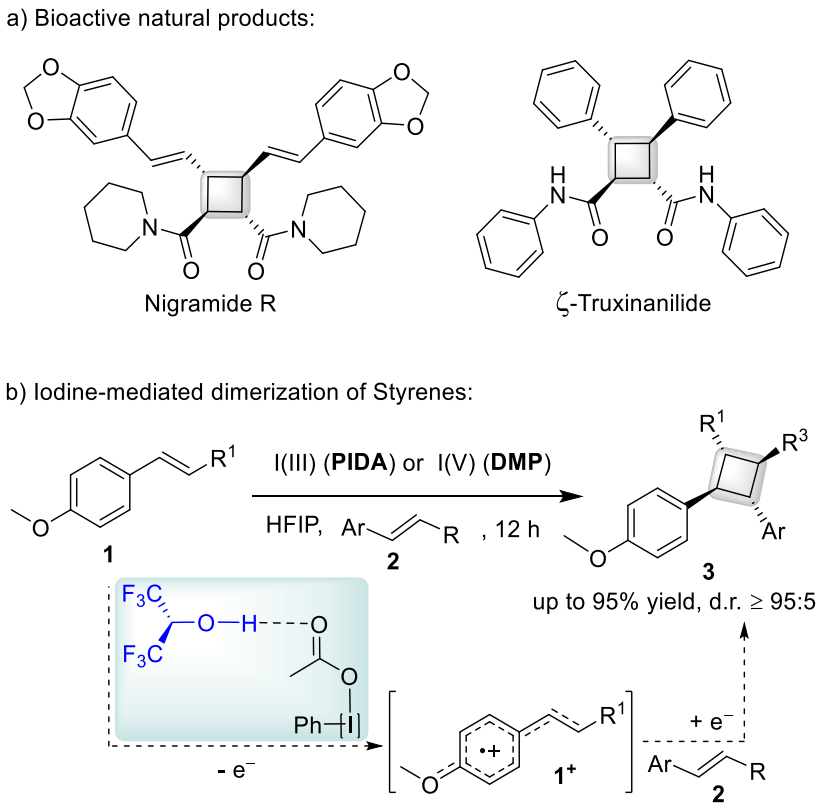

Figure 1. a) Examples of bioactive natural products containing cyclobutane ring. b) HOMD or HETD of styrenes with phenyliodine(III) diacetate (**PIDA**) or Dess-Martin periodinane (**DMP**), respectively .

The existence of hydrogen bonding interactions between the HFIP and **PIDA** has been proposed to be essential and the physical origin of the enhanced oxidative strength for the iodine reagent.[43] In addition to the almost disappearance of HO signals from NMR experiments, the voltammetric peak potential experiments measured versus Fc/Fc^{+} demonstrated a shift in reduction potentials for **PIDA** ($E_{p,c}$ in ACN = −1.32 V, $E_{p,c}$ in HFIP = −0.47 V). The possibility of ligand exchange between HFIP and **PIDA** has been excluded and any altered reactivity to the oxidants is ruled out as the HFIP is a low nucleophilic solvent.[43-47] All of the above-mentioned study concerns the first step of the reaction, the SEO step, and seems to us in need for further understandings despite the subsequent steps that lead to the all *trans* cyclobutane ring are not considered, at least to the best of our knowledge, by other workers under these conditions.[26, 48-50] An important question that should be raised is the number of electrons to be transferred to the iodine reagent to initiate the reaction. At this point, the reaction mechanism and reactivity of HVIR-mediate dimerization exclusively appears incomplete and warrants further attentions (Figure 2). Therefore, we herein interpret DFT simulations on the HOMD and HETD that gives all

trans cyclobutane under HVIRs with **PIDA** and **DMP**, respectively, featuring (1) the nature of initiation whether one or two electron reduction, (2) the effect of HFIP on reactivity of this protocol, and (3) realizing the dynamical nature of homo- and heterodimerization via quasiclassical trajectory molecular dynamics (QCTMD) simulations.

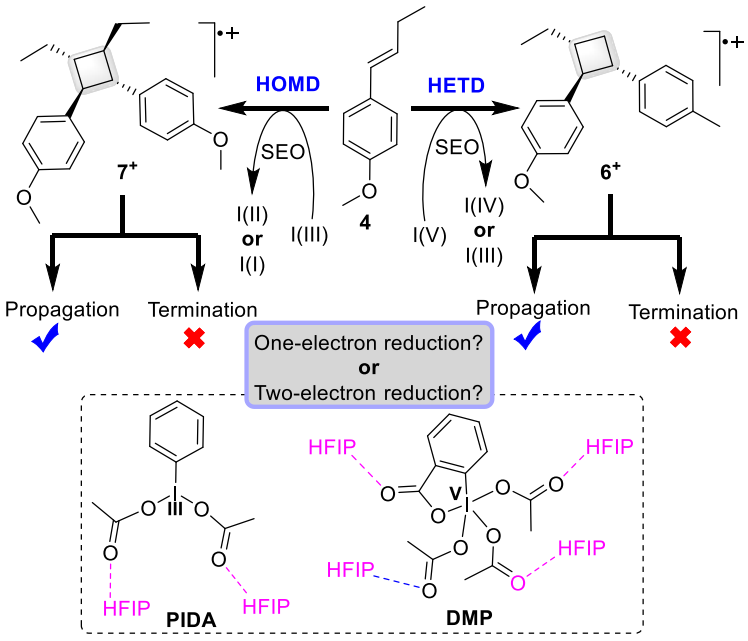

Figure 2. General representation of the HVIR [2+2] cycloaddition considered in this study, where iodine reagents are hydrogen bonded to HFIP explicitly.

Results and Discussion

To explore our HVIR-mediated dimerization of styrenes, we have divided our discussions into five distinct sections with the following order: validation of our strategy, mechanism of dimerization, molecular dynamics of HOMD and HETD.

Validation of strategy and level of theory

The calculations were conducted in explicit and implicit HFIP. The explicit HFIP protocol means that every single acetate groups in **PIDA** and **DMP** is hydrogen bonded to one HFIP molecule to match the experimental conditions, whereas the implicit protocol is performed only with continuum solvation model based on density

(IEFPCM-SMD). All structures were initially calculated using the *w*B97XD/6-311+G(d,p)/LANL2DZ//6-31G(d)/LANL2DZ level of theory, however we found inconsistencies with the experimental results because of Fe and I atoms. Therefore, we carried out a basis set search on Fe and I atoms through running single point energy calculations on optimized structure by 6-31G(d)/LANL2DZ through comparison between measured and calculated voltammetric peak potentials for redox species of different substituted *trans-β*-methylstyrenes toward **PIDA** (Figure 10, see below). For Fc/Fc^+, as shown in SI, the cyclopentadienyl group in Fc was tested with a basis set of triple- ζ quality (6-31G(d,p)) to be consistent with the valence basis sets used for iron. We found that Def2-TZVPP/6-31G(d,p) level of theory gives the best agreement with the experimental redox potential values of different substituted *trans-β*-methylstyrenes using Cp_2Fe (calculated $E^{1/2}$ = 4.84 V) as reference to calculate their redox potentials (see Figure 10). For iodine in **PIDA**, it was found that the basis set Def2-TZVPP for iodine and 6-311+G(d,p) for C, H, and O atoms gave the best agreement with experimental redox potentials (see SI). Importantly, and under explicit protocol, the calculated value for $\mathbf{PIDA_{HFIP}} + e^- \rightarrow \mathbf{PIDA^-_{HFIP}}$ is $E^{1/2}$ = 4.25 V of peak potential for $\mathbf{PIDA_{HFIP}}$ is $E_{p,c} = -0.59$ V versus calculated peak potential Fc/Fc^+ ($E^{1/2}$ = 4.84 V) as a reference, leading to a good agreement with the measured peak potential for **PIDA** is $E_{p,c} = -0.47$ V. Under implicit protocol, the calculated value of non-hydrogen-bonded **PIDA** is $E^{1/2}$ = 4.02 V of peak potential $E_{p,c} = -0.82$ V versus Fc/Fc^+ with a shifting to more negative value of 230 mV less favorable than explicit $\mathbf{PIDA_{HFIP}}$. Using this strategy, a good agreement between the measured and calculated peak potential have been achieved as shown in Figure 10. Therefore, the *w*B97XD/def2-TZVPP/6-311+G(d) level of theory is used for oxidants whereas the *w*B97XD/def2-TZVPP/6-31G(d,p) level of theory is utilized for Cp_2Fe in order to calculate the redox potentials. Comparison between calculated and measured redox potentials of different substituted *trans-β*-methylstyrenes **4a** – **4k** is indicated in Figure 3. Our strategic DFT simulations present a very good agreement with the experimental redox potentials and free energy of reoxidation accordingly. The explicit-involved HFIP calculations are consistent with experimental results than inexplicit calculations (for comparison see SI). The calculated results appeared in Figure 3-b indicate a deviation from experimental values of around 0.12 eV which is in agreement with the mean absolute error in ionization energy (2.74 kcal mol^{-1}) reported for *w*B97XD.[51]

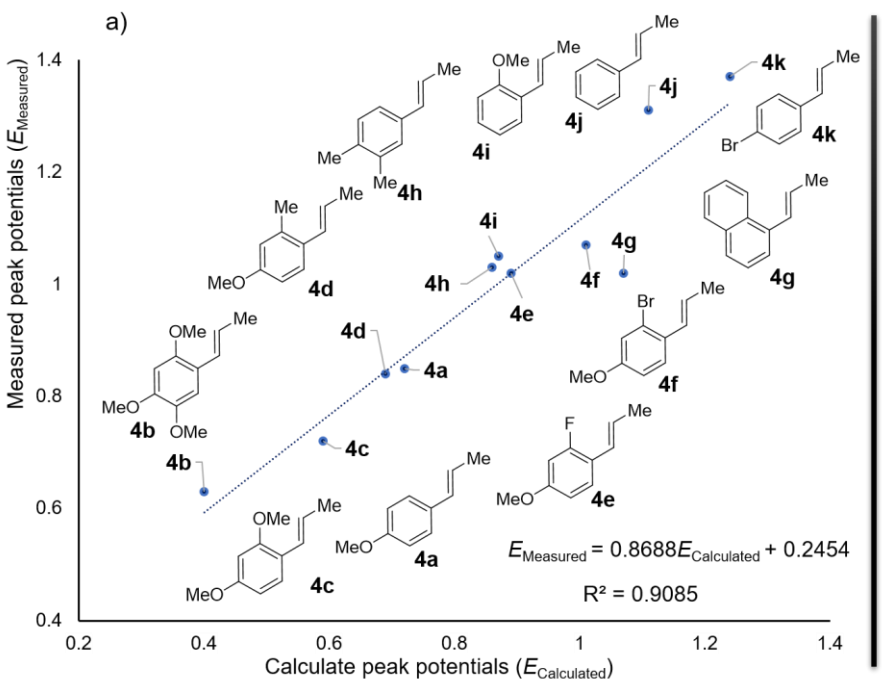

b)

	Measured		Calculated	
Subs.	$\Delta E_{p\text{-}p}$	$\Delta G°$	$\Delta E_{p\text{-}p}$	$\Delta G°$
4a	−1.31	30.2	−1.20	27.7
4b	−1.10	25.4	−0.88	20.3
4c	−1.19	27.4	−1.07	24.7
4d	−1.31	30.2	−1.17	27.0
4e	−1.49	34.4	−1.37	31.6
4f	−1.54	35.5	−1.49	34.4
4g	−1.49	34.4	−1.55	35.7
4h	−1.50	34.6	−1.34	30.9
4i	−1.52	35.1	−1.35	31.1
4j	−1.78	41.0	−1.60	36.9
4k	−1.84	42.4	−1.72	39.7

Figure 3. (a) Agreement between measured and calculated voltammetric peak potentials (in V) for redox species of different substituted *trans-β*-methylstyrenes **4a** – **4k**. (b) Differences in the reduction and oxidation peak potentials (in V) and their Gibbs free energies (in kcal mol^{-1}) for styrenes **4a** – **4k**. Styrenes **4g** – **4k** did not undergo **PIDA** [2+2] cycloaddition. The measured results were obtained versus Fc/Fc^{+}, as measured at 100 mV s^{-1}.[43] The calculated Fc/Fc^{+} is $E^{1/2}$ = 4.84 V in HFIP. The calculated value for **PIDA$_{HFIP}$** + e^{-} → **PIDA$^{-}_{HFIP}$** is $E^{1/2}$ = 4.25 V. Measured peak potential for **PIDA** is $E_{p,c}$ = −0.47 V.[43] Th calculated peak potential for **PIDA$_{HFIP}$** $E_{p,c}$ = −0.59 V.

Mechanism of dimerization

General Considerations. Our DFT investigations with the exploration of the HETD and HOMD facilitated by **DMP** and **PIDA**, respectively, are considered. Firstly, the cyclobutane ring formation is investigated based on the SEO and single electron reduction (SER). When the SEO and SER are initiated and terminated, respectively, through only HVIR to get cyclobutane ring formed, this is a catalytic mechanism. The more plausible scenario is that the HVIR only initiates the reaction to get the styrene molecule radicalized by SEO and propagation of the reaction proceeds without HVIR and this is an initiated or propagated mechanism as the HVIR serves as an initiator. Secondly, to account better knowledge about the height barrier of SEO, free energy of activation for

the SEO was calculated using four-point method proposed by Nelsen (see SI).[52-54] We are convinced that this method result in a reasonable estimation of the electron transfer (ET) activation barrier. Thirdly, it has been reported that HFIP plays a critical role with oxidizing agent rather than with the radical cation formed.[43] The effect of explicit hydrogen bonding in our calculations is considered only on the SEO steps, whereas the cyclization steps are proceeded with an implicit HFIP protocol.

HETD pathway. The DFT results of HETD in the presence I(V) **DMP** with and without explicit HFIP molecules have been exploited (for comparison between explicit and implicit HFIP see SI). Initially, the iodine catalyst undergoes either one-electron reduction to give I(IV) or two-electron reduction to give I(III), namely iodinane. Both pathways are investigated and shown in Figure 4. On one hand, when the initiation proceeds with a one-electron process, single electron transfer from one styrene to I(V), the free energy of activation for SEO for the FRS was found to be 20.2 kcal mol^{-1} to give radical cation $\mathbf{4}^{+}$ and radical anion $\mathbf{DMP}^{-}_{\mathbf{HFIP}}$ as an endergonic step (ΔG_r = 13.8 kcal mol^{-1}) (Figure 4). In absence of explicit HIFP the barrier for SEO increased to 25.4 kcal mol^{-1} as a more endergonic process (ΔG_r = 21.8 kcal mol^{-1}) (See SI). An apparent increased in the I–O bond distances, clearly represented for the perpendicular acetate units to the phenyl iodine. After the ET, the I–O bond distances elongate from 2.08 and 2.15 Å to 2.63 Å and 2.99 Å when HFIP are not involved in calculations explicitly (see **DMP** and **DMP**$^{-}$ in Figure xx). Elongation is slightly less when HFIP is involved explicitly, where I–O bond length is 2.12 Å is before the SEO and 2.55 Å and 2.77 Å are after the SEO (see $\mathbf{DMP}_{\mathbf{HFIP}}$ and $\mathbf{DMP}^{-}_{\mathbf{HFIP}}$ in Figure 4). On the other hand, a lower and more favored energetic pathway was found when a two-electron reduction process is involved, accompanying by two I─O bond cleavages, occurring through two SEOs from two styrenes give iodinane I(III) and two acetate groups stabilized by strong hydrogen bonding interactions (see $\mathbf{Iodinane \bullet 2AcO}^{-}_{\mathbf{HFIP}}$ in Figure 4). This pathway is lower than one-electron pathway by more than 7.0 kcal mol^{-1}. Here, addition of two electrons from two styrenes found to need only 5.4 kcal mol^{-1} as a free energy of reduction. Similarly, the change in oxidation state I(V)→I(III) has been reported for oxidation of alcohols to give iodinane and two acetic acid molecules.[55-57]

All trails to find a concerted [2+2] cycloaddition TS for the cation cyclobutane formation $\mathbf{6}^{+}$ are unsuccessful and, therefore, a two-step mechanism have been taken through the stepwise cycloaddition. For the first C-C bond formation, the head-to-head first C–C bond formation was found to have a barrier of 8.3 kcal mol^{-1} via

TS $\mathbf{8}^+$ with bond length of 2.20 Å along the TS is established, giving uncyclized intermediate $\mathbf{9}^+$ with C–C bond being formed at 1.58 Å as a thermoneutral step of 0.1 kcal mol^{-1} (Figure 3).[58] The TS $\mathbf{8}^+$ shows a π-π stacking interaction of 3.6 Å. A higher barrier TS of 13.1 kcal mol^{-1} was found without π-π stacking (see Figure SIxx). It seems that the favorable π-π stacking plays an important role in controlling the configurations of the product to be all *trans* cyclobutane. The presence of non-covalent interaction, π-π stacking, for TS $\mathbf{8}^+$ and intermediate $\mathbf{9}^+$ is shown by Reduced Density Gradient (RDG) analysis (see Figure SIxx).[59] Attractive π-π interaction is clearly seen in the green areas between the two phenyl rings. The nature of interaction between $\mathbf{4}^+$ and **5** through TS $\mathbf{8}^+$ has a radical character due to SOMO-HOMO overlapping. The SOMO orbitals located on radical styrene $\mathbf{4}^+$ is overlapped with the HOMOs of **5** with an energy gap if 4.03 eV (see Figure SIxx). The radical cation intermediate $\mathbf{9}^+$ cyclizes to the cationic cyclobutane $\mathbf{6}^+$ in a low barrier step of $\Delta G^{\ddagger}$ = 7.1 kcal mol^{-1} with a long C—C bond of 2.74 Å along TS $\mathbf{10}^+$ but in a slightly exergonic step (ΔG_r = −2.1 kcal mol^{-1}). Noticeably, the new C–C bond formed in cyclobutane $\mathbf{6}^+$ is 1.64 Å whereas all other C–C bonds in the ring are 1.54 Å, and this is attributed to radical character as indicated by the partial delocalization shown by spin density and β-LUMO contours (see Figure SIxx). To release the cyclobutane **6**, the radical cation $\mathbf{6}^+$ undergoes SER by or another styrene to propagate the reaction. The oxidation of styrene **4** by $\mathbf{6}^+$ is nearly to be barrierless of 1.1 kcal mol^{-1} as an exergonic step (ΔG_r = −6.6 kcal mol^{-1}) (Figure 4).

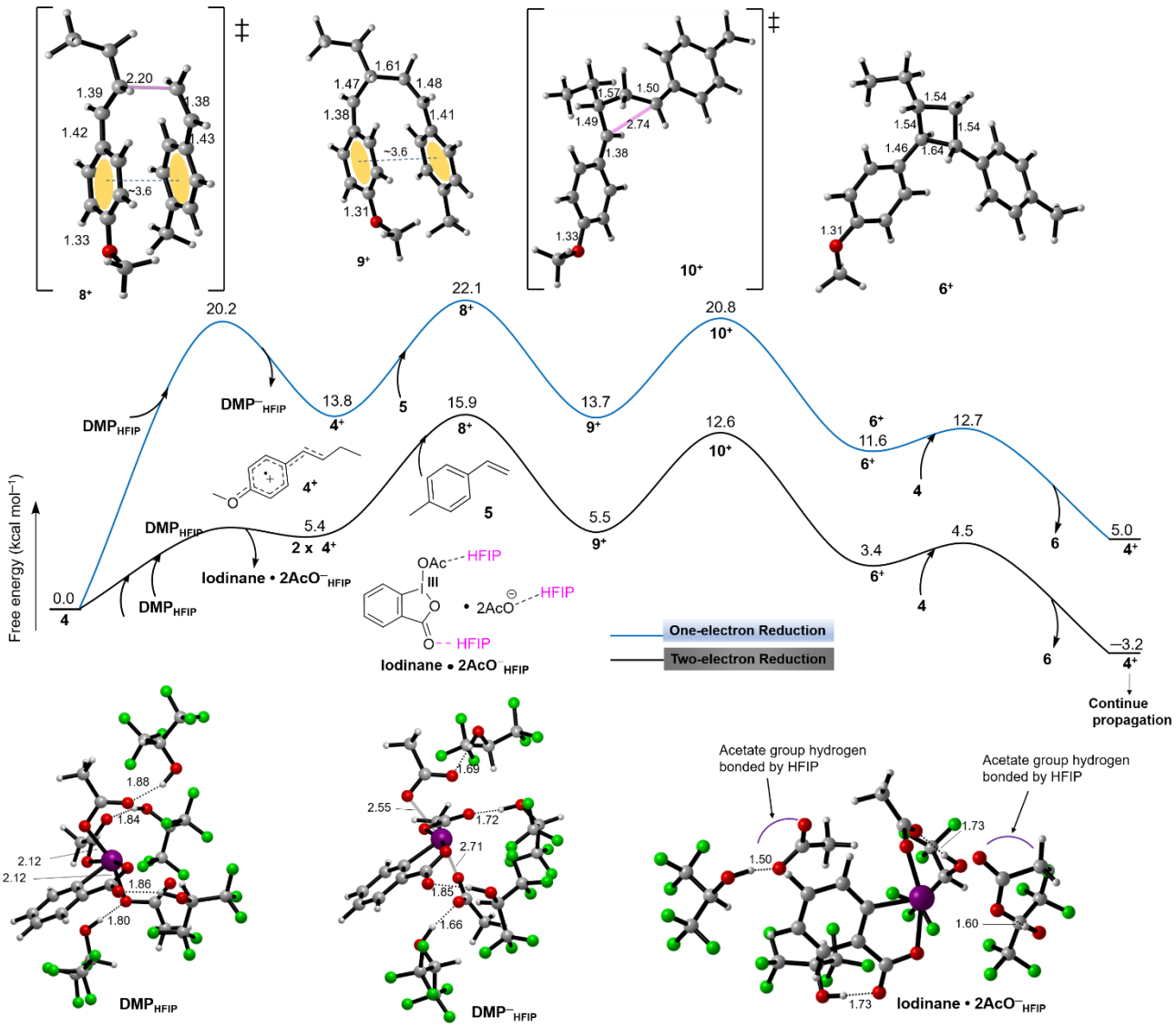

Figure 4. Free energy profile for the mechanism of **DMP**-mediated heterodimerization of styrenes (**4**) and (**5**) to yield cyclobutane **6** under one-electron reduction (blue pathway) and two-electron reduction (black pathway) hydrogen-bonded with HFIP.

HOMD pathway. Following the same strategy for HETD, the HOMD mechanism in the presence I(III) **PIDA** is investigated and shown in Figure 5. Under single electron reductive initiation, the barrier of SEO, the FRS, was found to be 31.3 kcal mol^{-1} to give radical cation **4**$^{+}$ and anion **PIDA**$^{-}_{\mathbf{HFIP}}$ as an endergonic step (ΔG_r = 28.1 kcal mol^{-1}). The SEO for HOMD is more endergonic than for the HETD. The calculated endergonicity for initiation by **PIDA$_{\mathbf{HFIP}}$** is in excellent agreement with that measured for *trans* anethol **14** (see Figure 3).[43] Following the SEO step the bond length of the acetate group to iodine, namely I–O bonds, increases from 2.15

Å to around 2.58 Å for the non-hydrogen bonded **PIDA** (Figure SIxx) and to longer distances of 2.66 Å and 2.78 Å for the hydrogen-bonded one $\mathbf{PIDA_{HFIP}}$ (Figure 5) for the reason mentioned above for SEO by $\mathbf{DMP_{HFIP}}$. However, when a reductive cleavage process, two-electron reduction, iodobenzene and two acetate groups stabilized by HFIP ($\mathbf{Iodobenzene \bullet 2AcO^{-}_{HFIP}}$) as well as two cationic styrenes are produced in a less endergonicity step of 21.4 kcal mol^{-1}. Comparison of one and two electron process initiations, the impact is substantially effective for **PIDA**-HOMD protocol in comparison to **DMP**-HETD protocol. The synthetic utility with **PIDA**/HFIP is considered to be mild conditions and the one-electron reduction would be highly unlikely and, therefore, two-electron process is required to initiate the radically-cationic [2+2] cycloaddition reaction. Reported literatures have shown that I(III), PIDA, undergoes a reductive cleavage of their I-O bonds under to yield the corresponding I(I), namely iodobenzene.[60] This has been also reported for oxidative of alcohols.[44]

The process for $\mathbf{4^{+}}\rightarrow\mathbf{12^{+}}$ has a reasonable barrier of 9.5 kcal mol^{-1} via π-π stacked head-to-head TS $\mathbf{11^{+}}$ with bond length of 2.16 Å to give the cationic uncyclized intermediate $\mathbf{12^{+}}$ as an endergonic step of 4.3 kcal mol^{-1} (Figure 5).[58] The favorable non-covalent interaction that represents the π-π stacking interaction between the two phenyl rings is shown in Figure SIxx. A higher barrier TS of 12.9 kcal mol^{-1} was found for the first C-C bond formation when aromatic rings are not stacked (Figure SIxx). Likely to TS $\mathbf{8^{+}}$, TS $\mathbf{11^{+}}$ has a radical character with an energy gap of 4.86 eV (see Figure SIxx) which is higher than for the HETD ($\mathbf{4^{+}}$ and **5**). The first C–C bond formation in $\mathbf{12^{+}}$ is longer than for that found for the uncyclized heterodimerized intermediate $\mathbf{9^{+}}$. The cyclization, TRS, is a low barrier step of 4.3 kcal mol^{-1} through TS $\mathbf{13^{+}}$ with C—C bond at 2.16 Å is seen to give the cationic homodimerized cyclobutane $\mathbf{7^{+}}$ as an exergonic step ($\mathbf{12^{+}}\rightarrow\mathbf{7^{+}}$, $\Delta G_r = -5.3$ kcal mol^{-1}, Figure 5). Upon formation of $\mathbf{7^{+}}$, the unpaired electron has totally delocalized over the entire system of $\mathbf{7^{+}}$ (see Figure SIxx) and resulted in an increase in the new C–C bond to be 1.71 Å, being longer than for $\mathbf{6^{+}}$. The release of neutral homodimerized cyclobutane **7** via propagation process (Figure 5) is calculated to be kinetically and thermodynamically favored. The oxidation of styrene **4** by $\mathbf{7^{+}}$ is found to be nearly barrierless of 1.5 kcal mol^{-1} as an exergonic step ($\Delta G_r = -6.3$ kcal mol^{-1}) in order to propagate the reaction.

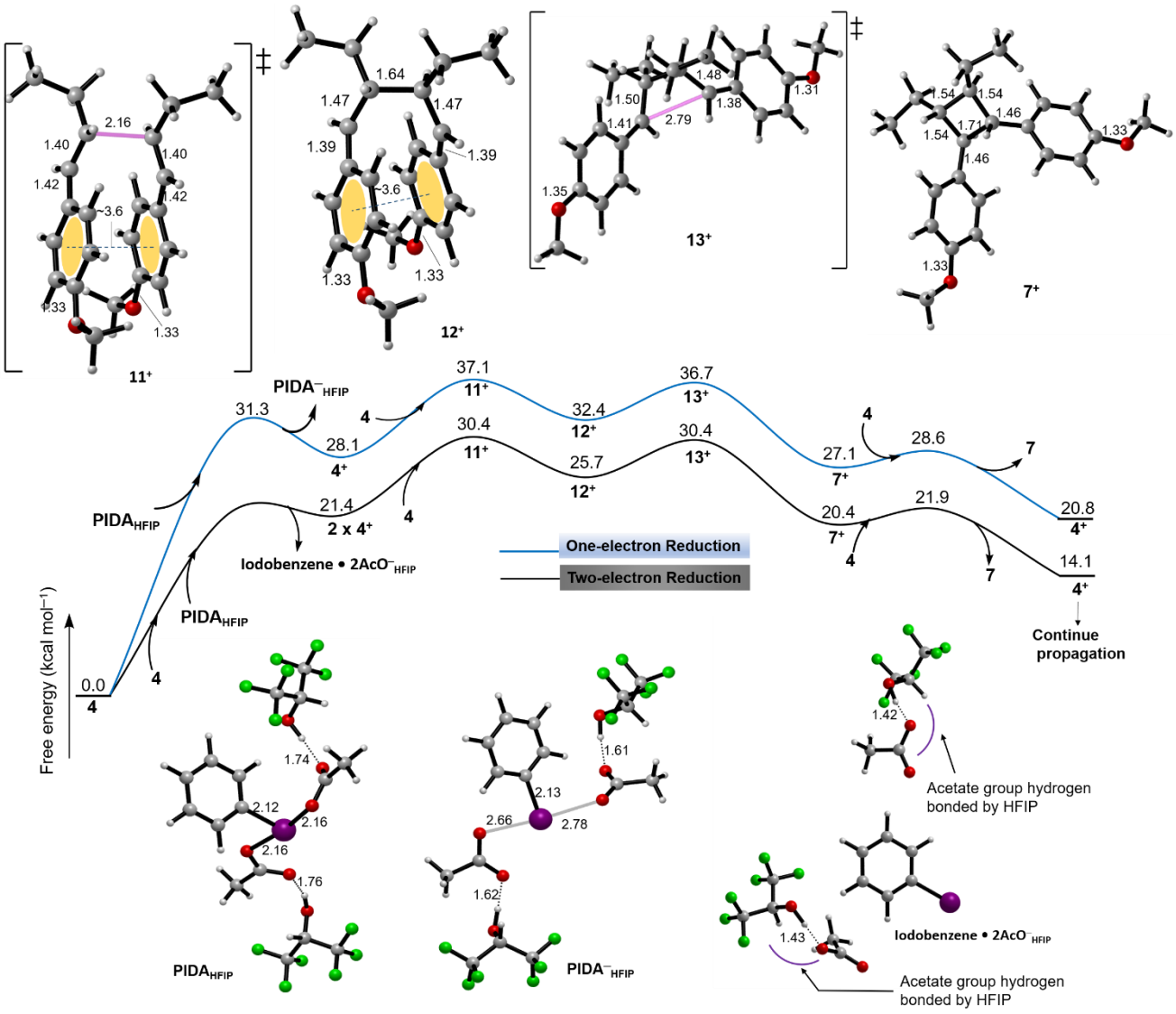

Figure 5. Free energy profile for the mechanism of **PIDA**-mediated heterodimerization of styrenes (**4**) to yield cyclobutane **7** under one-electron reduction (blue pathway) and two-electron reduction (black pathway) hydrogen-bonded with HFIP.

Molecular dynamics of HETD and HOMD

In general, the initiative SEO step from styrene **4** is shown to be more reactive with **DMP** catalyst since the SEO occurs with the more deficient catalyst I(V) (LUMO = –1.56 eV) over less deficient one I(III) (LUMO = –0.73 eV) (see Figure SIxx), apparently indicating that the initiation in HETD is faster than HOMD under **DMP** conditions. However, and from a synthetically perspective point of view, there is a relative competition between

both processes which is experimentally seen (see SI for ref 41).[41] The calculations indicate that once the radical cation $\mathbf{4}^+$ is formed, entering homo [2+2] cycloaddition is relatively possible. The results above (Figure 4 and 5) reveal that the HOMD starts with a barrier of 9.5 kcal mol^{-1} via TS $\mathbf{11}^+$ whereas HETD starts with lower barriers of 8.3 kcal mol^{-1} via TS $\mathbf{8}^+$, implying a barrier difference of $\Delta\Delta G^{\ddagger}$ = 1.2 kcal mol^{-1}. This refers to that the HETD is comparingly predominant. This is in general good agreement with the experimental findings, in which the HETD reaction proceeds an equivalent ratio of styrenes **5** to **4** of 2:1. A further evidence for the competition between HOMD and HETD is emerged form QCT molecular dynamics of the first C–C bond formation (shown below).

Quasiclassical trajectory molecular dynamics (QCTMD) simulations were utilized to understand the chronological character for formation of first C–C bonds in the HETD and HOMD (Figure 7).[61-67] The QCTMD simulations were carried out using the PROGDYN program, [68] a script suite that works in combination with Gaussian 09. 44 and 63 trajectories were generated starting from the TSs $\mathbf{8}^+$ and $\mathbf{11}^+$, respectively, in which forward and backward propagations (t = 0 fs) are initiated showing the typical reactive bonds toward either cationic uncyclized intermediates ($\mathbf{9}^+$ and $\mathbf{12}^+$) or reactants (styrene $\mathbf{4}^+$, **4** and **5**). No recrossing is observed in our simulation. The C3–C4 distance is rapidly shortened to ~1.6 Å in most trajectories, and the bond remains in the whole trajectory once formed although for a small proportion of trajectories the C3–C4 distance oscillates in the range between 1.6 Å and 2.0 Å. By recording the timing for the C3–C4 distance to be shortened below 1.6 Å, we obtained the average timing for the first C–C bond formation at 43.0 and 47.0 fs for HETD $\mathbf{8}^+$ and HOMD $\mathbf{11}^+$, respectively. It is interesting that although the average timing is similar, there are more trajectories exhibiting larger timing for C–C bond formation for the HOMD pathway, which may indicate a flatter potential energy surface in the post-transition state period. Comparison of the average time for the first C–C bond formation through TS $\mathbf{8}^+$ and TS $\mathbf{11}^+$ reveals a short timing gap of 4.0 fs. Also, the timing for first C–C bond formation for the unstacked TSs were obtained and shown a short timing gap where 46 fs for HOMD, derived from 24 trajectories, and 44 fs for HETD, derived from 20 trajectories (see Figure SIxx in SI). Overall, the very small timing gap between both pathways explains that HETD and HOMD are dynamically competitive.

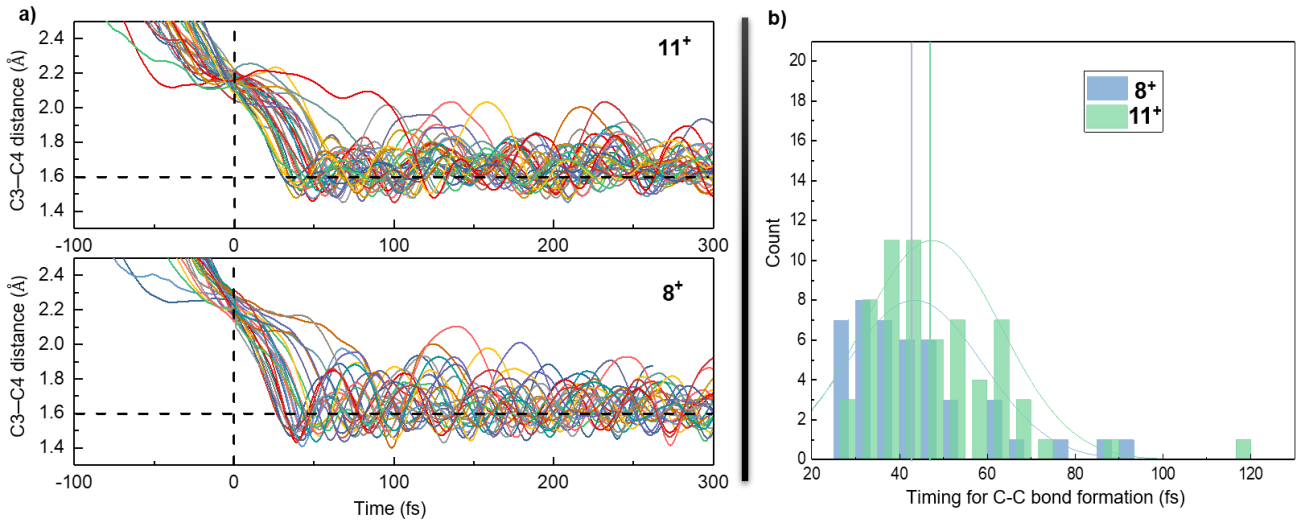

Figure 7. (a) Evolution of the C–C distance corresponding to the first C–C bond formation along quasiclassical trajectories initialized from TSs $\mathbf{8}^{+}$ and $\mathbf{11}^{+}$ calculated by the *w*B97XD/6-31G(d) level of theory. All trajectories start from the initial geometry (t = 0 fs) generated by adding a random displacement to the transition state, and both directions are shown in positive and negative part of the horizontal axis. (b) A histogram for the C–C bond formation timing, where the average timing for each reaction is shown by the vertical line.

Conclusions

DFT calculations at the (SMD)-*w*B97XD/Def2-TZVPP,6-311+G(d,p)//*w*B97XD/6-31G(d),LANL2DZ level of theory were exploited to provide mechanistic insights into the HVIR-promoted hetero- and homodimerizations of styrenes facilitated by HFIP. The computational level was validated through comparison between calculated and measured redox potentials of different substituted *trans*-*β*-methylstyrenes. The findings achieved in this study can be summarized as follows.

First, the hypervalent iodine-mediated hetero- and homodimerizations of styrenes initiated with two-electron reductive cleavage of two I─O bond cleavages giving iodinane I(III) and iodobenzene I(I) when **DMP** and **PIDA** are used, respectively, plus two acetate groups stabilized by strong hydrogen bonding interactions provided by HFIP. Accordingly, the propagation of the reaction is accomplished by radically-cationic hetero- and homodimerized cyclic intermediates. However, a disfavored initiation via a one-electron reduction was found, especially for the HOMD in the presence of **PIDA** where initiation become highly unlikely to take place.

This is agreement with the mild experimental conditions and, therefore, two-electron process is required to initiate the radically-cationic [2+2] cycloaddition reaction. Also, the change in oxidation state reported here, I(V)→I(III) and I(III)→I(I), are commensurate with the oxidation of alcohols by hypervalent iodine reagents.

Second. the mechanism of HETD and HOMD is a radically-characterized π-π stacked head-to-head stepwise [2+2] cycloaddition initiated via SEO by **DMP** and **PIDA**, respectively. DFT results supported by quasiclassical molecular dynamics simulations show that HOMD is dynamically competing pathway to HETD although the latter is relatively faster, in accordance with experimental observations.

Third, the rate-determining step was evaluated to be critical with I(III) to initiate the reaction as a thermodynamically endergonic whereas endergonicity from I(V) initiation showed to be very modest. The initiative SEO step was computed to be more reactive with **DMP** catalyst as the SEO occurs with the more deficient catalyst I(V) (lower LUMO) over less deficient one I(III) (higher LUMO).

Overall, this mechanistic study brings significantly important insights into a such influential synthetic utility and opens possibilities toward advancing an efficient protocol for stereoselective approaches of simple and complex hetero- and homodimerizations. We envision that using DFT simulations on catalyzed SEO will enhance and warrant further attentions toward developing various oxidants to synthetically access a wide range of substrates used for bioactive and synthetic cyclobutane-containing products in a more efficiently-controlled fashion.

ASSOCIATED CONTENT

Supporting Information

The Supporting Information is available free of charge on the ACS Publications website. Further computational results, absolute energies and cartesian coordinates (PDF)

AUTHOR INFORMATION

Corresponding Author

Aqeel A. Hussein - School of Chemistry, University of Southampton, Southampton, Hampshire, SO17 1BJ, United Kingdom; College of Dentistry, University of Al-Ameed, Karbala PO Box 198, Iraq; orcid.org/0000-0002-9259-9609; Email: aahh1f19@soton.ac.uk

Authors

Ahmed Al-Yasari - School of Chemistry, University of East Anglia, Norwich, NR4 7TJ, United Kingdom; Department of Chemistry, Faculty of Sciences, University of Kerbala, Kerbala, Iraq; orcid.org/0000-0001-8768-1248

Yumiao Ma - BSJ Institute, Haidian, Beijing, 100084, People's Republic of China; orcid.org/0000-0002-0628-8864

Author Contributions

‡These authors contributed equally.

Notes

The authors declare no competing financial interest.

Acknowledgements

The authors acknowledge the computational resources from the iridis4 supercomputer supported by the University of Southampton. A.A.H. highly acknowledge the University of Southampton/School of Chemistry for providing the visitor-status research position (2717441/EB00-VISIT). A.A.H. thanks Prof. Richard C. D. Brown for his valuable support.

References

1. Xu, Y.; Conner, M. L.; Brown, M. K., Cyclobutane and Cyclobutene Synthesis: Catalytic Enantioselective 2+2 Cycloadditions. *Angewandte Chemie-International Edition* **2015,** *54* (41), 11918-11928.
2. Margaretha, P., Retrospective View on Recent Developments in Cyclobutane Synthesis via [2+2] Photocycloaddition of Unsaturated Ketones to Acyclic Dienes. *Helvetica Chimica Acta* **2014,** *97* (7), 1027-1035.

3. Dembitsky, V. M., Naturally occurring bioactive Cyclobutane-containing (CBC) alkaloids in fungi, fungal endophytes, and plants. *Phytomedicine* **2014,** *21* (12), 1559-1581.
4. Dembitsky, V. M., Bioactive cyclobutane-containing alkaloids. *Journal of Natural Medicines* **2008,** *62* (1), 1-33.
5. Cretton, S.; Bartholomeusz, T. A.; Jeannerat, D.; Munoz, O.; Christen, P.; Hostettmann, K., New cyclobutane-containing tropane alkaloids from the aerial parts of Schizanthus grahamii. *Planta Medica* **2009,** *75* (9), 916-916.
6. Ito, H.; Toyoda, T.; Sawamura, M., Stereospecific Synthesis of Cyclobutylboronates through Copper(I)-Catalyzed Reaction of Homoallylic Sulfonates and a Diboron Derivative. *Journal of the American Chemical Society* **2010,** *132* (17), 5990-5992.
7. Noucti, N. N.; Alexanian, E. J., Stereoselective Nickel- Catalyzed 2+2 Cycloadditions of EneAllenes. *Angewandte Chemie-International Edition* **2015,** *54* (18), 5447-5450.
8. Gulías, M.; Collado, A.; Trillo, B.; López, F.; Oñate, E.; Esteruelas, M. A.; Mascareñas, J. L., Ruthenium-Catalyzed (2 + 2) Intramolecular Cycloaddition of Allenenes. *Journal of the American Chemical Society* **2011,** *133* (20), 7660-7663.
9. Luzung, M. R.; Mauleón, P.; Toste, F. D., Gold(I)-Catalyzed [2 + 2]-Cycloaddition of Allenenes. *Journal of the American Chemical Society* **2007,** *129* (41), 12402-12403.
10. Chiba, K.; Miura, T.; Kim, S.; Kitano, Y.; Tada, M., Electrocatalytic Intermolecular Olefin Cross-Coupling by Anodically Induced Formal [2+2] Cycloaddition between Enol Ethers and Alkenes. *Journal of the American Chemical Society* **2001,** *123* (45), 11314-11315.
11. Rath, B. B.; Kole, G. K.; Morris, S. A.; Vittal, J. J., Rotation of a helical coordination polymer by mechanical grinding. *Chemical Communications* **2020**.
12. Ledwith, A., Cation radicals in electron transfer reactions. *Accounts of Chemical Research* **1972,** *5* (4), 133-139.
13. Bell, F. A.; Crellin, R. A.; Fujii, H.; Ledwith, A., Cation-radicals: metal-catalysed cyclodimerisation of aromatic enamines. *Journal of the Chemical Society D: Chemical Communications* **1969,** (6), 251-252.
14. Bauld, N. L.; Bellville, D. J.; Harirchian, B.; Lorenz, K. T.; Pabon, R. A.; Reynolds, D. W.; Wirth, D. D.; Chiou, H. S.; Marsh, B. K., Cation radical pericyclic reactions. *Accounts of Chemical Research* **1987,** *20* (10), 371-378.
15. Bauld, N. L.; Bellville, D. J.; Pabon, R.; Chelsky, R.; Green, G., Theory of cation-radical pericyclic reactions. *Journal of the American Chemical Society* **1983,** *105* (8), 2378-2382.
16. Bauld, N. L.; Pabon, R., Cation radical catalyzed olefin cyclodimerization. *Journal of the American Chemical Society* **1983,** *105* (3), 633-634.
17. Ischay, M. A.; Ament, M. S.; Yoon, T. P., Crossed intermolecular [2 + 2] cycloaddition of styrenes by visible light photocatalysis. *Chemical Science* **2012,** *3* (9), 2807-2811.
18. Riener, M.; Nicewicz, D. A., Synthesis of cyclobutane lignans via an organic single electron oxidant–electron relay system. *Chemical Science* **2013,** *4* (6), 2625-2629.
19. Jiang, Y.; Wang, C.; Rogers, C. R.; Kodaimati, M. S.; Weiss, E. A., Regio- and diastereoselective intermolecular [2+2] cycloadditions photocatalysed by quantum dots. *Nature Chemistry* **2019,** *11* (11), 1034-1040.
20. Ischay, M. A.; Lu, Z.; Yoon, T. P., [2+2] Cycloadditions by Oxidative Visible Light Photocatalysis. *Journal of the American Chemical Society* **2010,** *132* (25), 8572-8574.
21. Lu, Z.; Yoon, T. P., Visible Light Photocatalysis of [2+2] Styrene Cycloadditions by Energy Transfer. *Angewandte Chemie International Edition* **2012,** *51* (41), 10329-10332.
22. Hurtley, A. E.; Lu, Z.; Yoon, T. P., [2+2] Cycloaddition of 1,3-Dienes by Visible Light Photocatalysis. *Angewandte Chemie International Edition* **2014,** *53* (34), 8991-8994.
23. Fleming, S. A.; Ward, S. C., Stereocontrolled photochemical [2 + 2] cycloaddition. *Tetrahedron Letters* **1992,** *33* (8), 1013-1016.
24. Ward, S. C.; Fleming, S. A., [2 + 2] Photocycloaddition of Cinnamyloxy Silanes. *The Journal of Organic Chemistry* **1994,** *59* (21), 6476-6479.
25. Horibe, T.; Katagiri, K.; Ishihara, K., Radical-Cation-Induced Crossed [2+2] Cycloaddition of Electron-Deficient Anetholes Initiated by Iron(III) Salt. *Advanced Synthesis & Catalysis* **2020,** *362* (4), 960-963.
26. Zhao, L.-M.; Lei, T.; Liao, R.-Z.; Xiao, H.; Chen, B.; Ramamurthy, V.; Tung, C.-H.; Wu, L.-Z., Visible-Light-Triggered Selective Intermolecular [2+2] Cycloaddition of Extended Enones: 2-Oxo-3-enoates and 2,4-Dien-1-ones with Olefins. *The Journal of Organic Chemistry* **2019,** *84* (14), 9257-9269.
27. Li, R.; Ma, B. C.; Huang, W.; Wang, L.; Wang, D.; Lu, H.; Landfester, K.; Zhang, K. A. I., Photocatalytic Regioselective and Stereoselective [2 + 2] Cycloaddition of Styrene Derivatives Using a Heterogeneous Organic Photocatalyst. *ACS Catalysis* **2017,** *7* (5), 3097-3101.
28. Amjaour, H.; Wang, Z.; Mabin, M.; Puttkammer, J.; Busch, S.; Chu, Q. R., Scalable preparation and property investigation of a cis-cyclobutane-1,2-dicarboxylic acid from β-trans-cinnamic acid. *Chemical Communications* **2019,** *55* (2), 214-217.
29. Yoshimura, A.; Zhdankin, V. V., Advances in Synthetic Applications of Hypervalent Iodine Compounds. *Chemical Reviews* **2016,** *116* (5), 3328-3435.

30. Li, Y.; Hari, D. P.; Vita, M. V.; Waser, J., Cyclic Hypervalent Iodine Reagents for Atom-Transfer Reactions: Beyond Trifluoromethylation. *Angewandte Chemie International Edition* **2016,** *55* (14), 4436-4454.
31. Colomer, I.; Chamberlain, A. E. R.; Haughey, M. B.; Donohoe, T. J., Hexafluoroisopropanol as a highly versatile solvent. *Nature Reviews Chemistry* **2017,** *1* (11), 0088.
32. Zhu, Y.; Colomer, I.; Thompson, A. L.; Donohoe, T. J., HFIP Solvent Enables Alcohols To Act as Alkylating Agents in Stereoselective Heterocyclization. *Journal of the American Chemical Society* **2019,** *141* (16), 6489-6493.
33. Colomer, I.; Barcelos, R. C.; Christensen, K. E.; Donohoe, T. J., Orthogonally Protected 1,2-Diols from Electron-Rich Alkenes Using Metal-Free Olefin syn-Dihydroxylation. *Organic Letters* **2016,** *18* (22), 5880-5883.
34. Raheem, I. T.; Thiara, P. S.; Peterson, E. A.; Jacobsen, E. N., Enantioselective Pictet−Spengler-Type Cyclizations of Hydroxylactams: H-Bond Donor Catalysis by Anion Binding. *Journal of the American Chemical Society* **2007,** *129* (44), 13404-13405.
35. Lv, H.; Zhan, J.-H.; Cai, Y.-B.; Yu, Y.; Wang, B.; Zhang, J.-L., π–π Interaction Assisted Hydrodefluorination of Perfluoroarenes by Gold Hydride: A Case of Synergistic Effect on C–F Bond Activation. *Journal of the American Chemical Society* **2012,** *134* (39), 16216-16227.
36. Doyle, A. G.; Jacobsen, E. N., Small-Molecule H-Bond Donors in Asymmetric Catalysis. *Chemical Reviews* **2007,** *107* (12), 5713-5743.
37. Nicolaou, K. C.; Baran, P. S.; Zhong, Y.-L.; Vega, J. A., Novel IBX-Mediated Processes for the Synthesis of Amino Sugars and Libraries Thereof. *Angewandte Chemie International Edition* **2000,** *39* (14), 2525-2529.
38. Nicolaou, K. C.; Baran, P. S.; Zhong, Y. L.; Barluenga, S.; Hunt, K. W.; Kranich, R.; Vega, J. A., Iodine(V) Reagents in Organic Synthesis. Part 3. New Routes to Heterocyclic Compounds via o-Iodoxybenzoic Acid-Mediated Cyclizations: Generality, Scope, and Mechanism. *Journal of the American Chemical Society* **2002,** *124* (10), 2233-2244.
39. Nicolaou, K. C.; Baran, P. S.; Kranich, R.; Zhong, Y.-L.; Sugita, K.; Zou, N., Mechanistic Studies of Periodinane-Mediated Reactions of Anilides and Related Systems. *Angewandte Chemie International Edition* **2001,** *40* (1), 202-206.
40. Janza, B.; Studer, A., Stereoselective Cyclization Reactions of IBX-Generated Alkoxyamidyl Radicals. *The Journal of Organic Chemistry* **2005,** *70* (17), 6991-6994.
41. Colomer, I.; Coura Barcelos, R.; Donohoe, T. J., Catalytic Hypervalent Iodine Promoters Lead to Styrene Dimerization and the Formation of Tri- and Tetrasubstituted Cyclobutanes. *Angewandte Chemie International Edition* **2016,** *55* (15), 4748-4752.
42. Zhu, Y.; Colomer, I.; Donohoe, T. J., Hypervalent iodine initiated intramolecular alkene dimerisation: a stereodivergent entry to cyclobutanes. *Chemical Communications* **2019,** *55* (69), 10316-10319.
43. Colomer, I.; Batchelor-McAuley, C.; Odell, B.; Donohoe, T. J.; Compton, R. G., Hydrogen Bonding to Hexafluoroisopropanol Controls the Oxidative Strength of Hypervalent Iodine Reagents. *Journal of the American Chemical Society* **2016,** *138* (28), 8855-8861.
44. Farshadfar, K.; Chipman, A.; Yates, B. F.; Ariafard, A., DFT Mechanistic Investigation into BF3-Catalyzed Alcohol Oxidation by a Hypervalent Iodine(III) Compound. *ACS Catalysis* **2019,** *9* (7), 6510-6521.
45. Ganji, B.; Ariafard, A., DFT mechanistic investigation into phenol dearomatization mediated by an iodine(iii) reagent. *Organic & Biomolecular Chemistry* **2019,** *17* (14), 3521-3528.
46. Kaur, A.; Ariafard, A., Mechanistic investigation into phenol oxidation by IBX elucidated by DFT calculations. *Organic & Biomolecular Chemistry* **2020,** *18* (6), 1117-1129.
47. De Munari, S.; Frigerio, M.; Santagostino, M., Hypervalent Iodine Oxidants: Structure and Kinetics of the Reactive Intermediates in the Oxidation of Alcohols and 1,2-Diols by o-Iodoxybenzoic Acid (IBX) and Dess−Martin Periodinane. A Comparative 1H-NMR Study. *The Journal of Organic Chemistry* **1996,** *61* (26), 9272-9279.
48. O'Nei, L. L.; Wiest, O., Acyclic or Long-Bond Intermediate in the Electron-Transfer-Catalyzed Dimerization of 4-Methoxystyrene. *The Journal of Organic Chemistry* **2006,** *71* (23), 8926-8933.
49. Guo, C.; Cui, L.; Chen, B.; Yuan, J.; Tian, Z., A theoretical study on the stereoconvergency of the intramolecular radical cation [2+2] cycloadditions of bis(styrenes). *RSC Advances* **2012,** *2* (26), 9932-9937.
50. Li, Y.; Guo, C.; Chen, B.-Z., A theoretical study on intermolecular [2+2] radical cation cycloaddition reactions and the competition between concerted and stepwise mechanisms. *Computational and Theoretical Chemistry* **2016,** *1078*, 163-172.
51. Chai, J.-D.; Head-Gordon, M., Long-range corrected hybrid density functionals with damped atom-atom dispersion corrections. *PCCP* **2008,** *10* (44), 6615-6620.
52. Nelsen, S. F.; Blackstock, S. C.; Kim, Y., Estimation of inner shell Marcus terms for amino nitrogen compounds by molecular orbital calculations. *Journal of the American Chemical Society* **1987,** *109* (3), 677-682.
53. Vaissier, V.; Barnes, P.; Kirkpatrick, J.; Nelson, J., Influence of polar medium on the reorganization energy of charge transfer between dyes in a dye sensitized film. *Physical Chemistry Chemical Physics* **2013,** *15* (13), 4804-4814.

54. Manke, F.; Frost, J. M.; Vaissier, V.; Nelson, J.; Barnes, P. R. F., Influence of a nearby substrate on the reorganization energy of hole exchange between dye molecules. *Physical Chemistry Chemical Physics* **2015,** *17* (11), 7345-7354.
55. Meyer, S. D.; Schreiber, S. L., Acceleration of the Dess-Martin Oxidation by Water. *The Journal of Organic Chemistry* **1994,** *59* (24), 7549-7552.
56. Dess, D. B.; Martin, J. C., A useful 12-I-5 triacetoxyperiodinane (the Dess-Martin periodinane) for the selective oxidation of primary or secondary alcohols and a variety of related 12-I-5 species. *Journal of the American Chemical Society* **1991,** *113* (19), 7277-7287.
57. Dess, D. B.; Martin, J. C., Readily accessible 12-I-5 oxidant for the conversion of primary and secondary alcohols to aldehydes and ketones. *The Journal of Organic Chemistry* **1983,** *48* (22), 4155-4156.
58. Demaille, C.; Bard, A. J., Kinetics and mechanism of the anodic dimerization of trans-anethole studied by cyclic voltammetry and scanning electrochemical microscopy. *Acta Chemica Scandinavica* **1999,** *53* (10), 842-848.
59. Johnson, E. R.; Keinan, S.; Mori-Sánchez, P.; Contreras-García, J.; Cohen, A. J.; Yang, W., Revealing Noncovalent Interactions. *Journal of the American Chemical Society* **2010,** *132* (18), 6498-6506.
60. Kokkinidis, G.; Hatzigrigoriou, E.; Sazou, D.; Varvoglis, A., Electrochemical reduction of some hypervalent iodine compounds. *Electrochimica Acta* **1991,** *36* (9), 1391-1395.
61. Burns, J. M.; Boittier, E. D., Pathway Bifurcation in the (4 + 3)/(5 + 2)-Cycloaddition of Butadiene and Oxidopyrylium Ylides: The Significance of Molecular Orbital Isosymmetry. *The Journal of Organic Chemistry* **2019**.
62. Villar López, R.; Faza, O. N.; Silva López, C., Dynamic Effects Responsible for High Selectivity in a [3,3] Sigmatropic Rearrangement Featuring a Bispericyclic Transition State. *The Journal of Organic Chemistry* **2017,** *82* (9), 4758-4765.
63. Patel, A.; Chen, Z.; Yang, Z. Y.; Gutierrez, O.; Liu, H. W.; Houk, K. N.; Singleton, D. A., Dynamically Complex 6+4 and 4+2 Cycloadditions in the Biosynthesis of Spinosyn A. *Journal of the American Chemical Society* **2016,** *138* (11), 3631-3634.
64. Xu, L.; Doubleday, C. E.; Houk, K. N., Dynamics of Carbene Cycloadditions. *Journal of the American Chemical Society* **2011,** *133* (44), 17848-17854.
65. Xu, L.; Doubleday, C. E.; Houk, K. N., Dynamics of 1,3-Dipolar Cycloadditions: Energy Partitioning of Reactants and Quantitation of Synchronicity. *Journal of the American Chemical Society* **2010,** *132* (9), 3029-3037.
66. Black, K.; Liu, P.; Xu, L.; Doubleday, C.; Houk, K. N., Dynamics, transition states, and timing of bond formation in Diels-Alder reactions. *Proceedings of the National Academy of Sciences of the United States of America* **2012,** *109* (32), 12860-12865.
67. Patel, A.; Chen, Z.; Yang, Z.; Gutiérrez, O.; Liu, H.-w.; Houk, K. N.; Singleton, D. A., Dynamically Complex [6+4] and [4+2] Cycloadditions in the Biosynthesis of Spinosyn A. *Journal of the American Chemical Society* **2016,** *138* (11), 3631-3634.
68. Singleton, D. A.; Hang, C.; Szymanski, M. J.; Greenwald, E. E., A New Form of Kinetic Isotope Effect. Dynamic Effects on Isotopic Selectivity and Regioselectivity. *Journal of the American Chemical Society* **2003,** *125* (5), 1176-1177.